Particuology 7 (2009) 220–224

Contents lists available at ScienceDirect

Particuology

journal homepage: www.elsevier.com/locate/partic

Short communication

Explicit solvent molecular dynamics simulations of chaperonin-assisted rhodanese folding

Ying Ren[a,b], Jian Gao[a,*], Ji Xu[a,b], Wei Ge[a], Jinghai Li[a]

[a] State Key Laboratory of Multiphase Complex System, Institute of Process Engineering, Chinese Academy of Sciences, Beijing 100190, China
[b] Graduate University of the Chinese Academy of Sciences, Beijing 100039, China

ARTICLE INFO

Article history:
Received 23 December 2008
Accepted 13 March 2009

Keywords:
Molecular dynamics simulation
Explicit solvent
Chaperonin-assisted
Protein folding
Molecular chaperonin
Rhodanese

ABSTRACT

Chaperonins are known to facilitate the productive folding of numerous misfolded proteins. Despite their established importance, the mechanism of chaperonin-assisted protein folding remains unknown. In the present article, all-atom explicit solvent molecular dynamics (MD) simulations have been performed for the first time on rhodanese folding in a series of cavity-size and cavity-charge chaperonin mutants. A compromise between stability and flexibility of chaperonin structure during the substrate folding has been observed and the key factors affecting this dynamic process are discussed.

1. Introduction

Extension of particle simulation methods like MD, discrete element method (DEM), pseudo particle modeling (PPM), macro-scale pseudo particle modeling (MaPPM) to different complex systems has paved a way for wider application in practical processes like bio-molecular systems and nano-materials (Ge et al., 2007; Ge & Li, 2001). Among them, protein folding, a fundamental process in living bodies, has attracted more and more attention. *In vivo*, protein folding is assisted by a set of proteins, collectively known as molecular chaperones, which help proteins fold successfully to their native structures in the crowded environment of a cell (Ellis, 2001). One of the most studied chaperonins is the bacterial chaperonin GroEL and its co-chaperonin GroES, that is, the so-called GroEL/ES complex. While its structure is now well characterized as two heptameric rings consisting of seven identical GroEL subunits each, with a dome-shaped heptameric ring consisting of seven identical GroES subunits on top of GroEL, the mechanism of chaperonin-mediated protein folding is still poorly understood. Current experimental techniques are very difficult to unravel the dynamics of the partially folded peptide inside the chaperonin with sufficient temporal and spatial resolutions, making discrete computer simulation a powerful tool to understand the problem at molecular level. However, due to computational limitations, most studies have relied on coarse-grained simulations using a rigid geometry with a homogeneous inner lining to represent the chaperonin and a rough model protein to represent the substrate (Jewett, Baumketner, & Shea, 2004; Klimov, Newfield, & Thirumalai, 2002; Takagi, Koga, & Takada, 2003), thus inevitably ignoring the true chemical characteristics of the cavity and the substrate protein. Implicit solvent models, though having the advantage of reducing computational powers, would incur tremendous errors by approximating the electrostatic properties of the discrete solvent as a dielectric continuum (Lin, Baker, & McCammon, 2002). The all-atom explicit solvent model would be the best choice for a detailed description of such investigations. Recently, with the help of our newly built high-performance computer system with a capacity of 100 T single-precision flops, we have performed the first all-atom explicit solvent MD simulations on this dynamic process for ~150 ns, which is also the longest so far as we know.

Bovine liver rhodanese (Protein Data Bank code 1RHD (Ploegman, Drent, Kalk, & Hol, 1978)), a 293-residue with a molecular weight of ~33 kD, has been widely investigated as a substrate for assisted folding by molecular chaperonin (Horowitz, 1995; Tang et al., 2006). Here, we carry out all-atom, explicit solvent, molecular dynamics simulations of a series of GroEL/ES mutants, and investigate two major physical properties: the size and the charge of the cavity. Only the cis-cavity of GroEL is included in the simulation since the trans-cavity plays no essential role in substrate folding (Tang et al., 2006) but costs tremendous computational time. As shown in Fig. 1, the C-terminus (the end of the amino acid chain terminated by a free carboxyl group) of each GroEL subunit

* Corresponding author. Tel.: +86 10 62555245; fax: +86 10 62558065.
E-mail address: jgao@home.ipe.ac.cn (J. Gao).

1674-2001/$ – see front matter © 2009 Chinese Society of Particuology and Institute of Process Engineering, Chinese Academy of Sciences. Published by Elsevier B.V. All rights reserved.
doi:10.1016/j.partic.2009.03.001

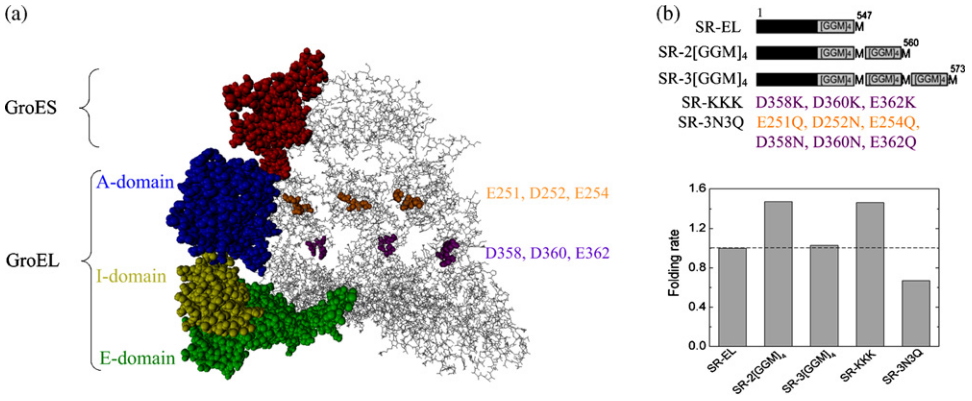

Fig. 1. (a) Architecture of GroEL/ES complex (PDB code 1AON (Xu, Horwich, & Sigler, 1997)) offering a view into the cis-cavity shown with four subunits of GroEL and GroES (only the cis-cavity is shown for clarity). Clusters of negatively charged residues exposed toward the cis-cavity are highlighted in orange (E251, D252, E254) and purple (D358, D360, E362). GroES, the A-domain, I-domain and E-domain of GroEL are shown in red, blue, yellow and green, respectively. (b, top), schematic representation of a series of GroEL; (b, bottom), corresponding experimental results of rhodanese folding rate (Tang et al., 2006), the dashed line representing the folding rate obtained with SR-EL set to 1.0. Nomenclature for the mutants is taken from the experimental work of Tang et al. (2006). (For interpretation of the references to color in this figure legend, the reader is referred to the web version of the article.)

Table 1
Details of all simulations performed.

System	GroEL construct	Cavity volume change (%)	Cavity net charge	No. of atoms
1	SR-EL	0	−42	350,618
2	SR-2[GGM]$_4$	−4.4	−42	350,157
3	SR-3[GGM]$_4$	−8.7	−42	350,146
4	SR-KKK	0	0	350,725
5	SR-3N3Q	0	0	350,741

Note: Nomenclature for mutants according to experimental work of Tang et al. (2006).

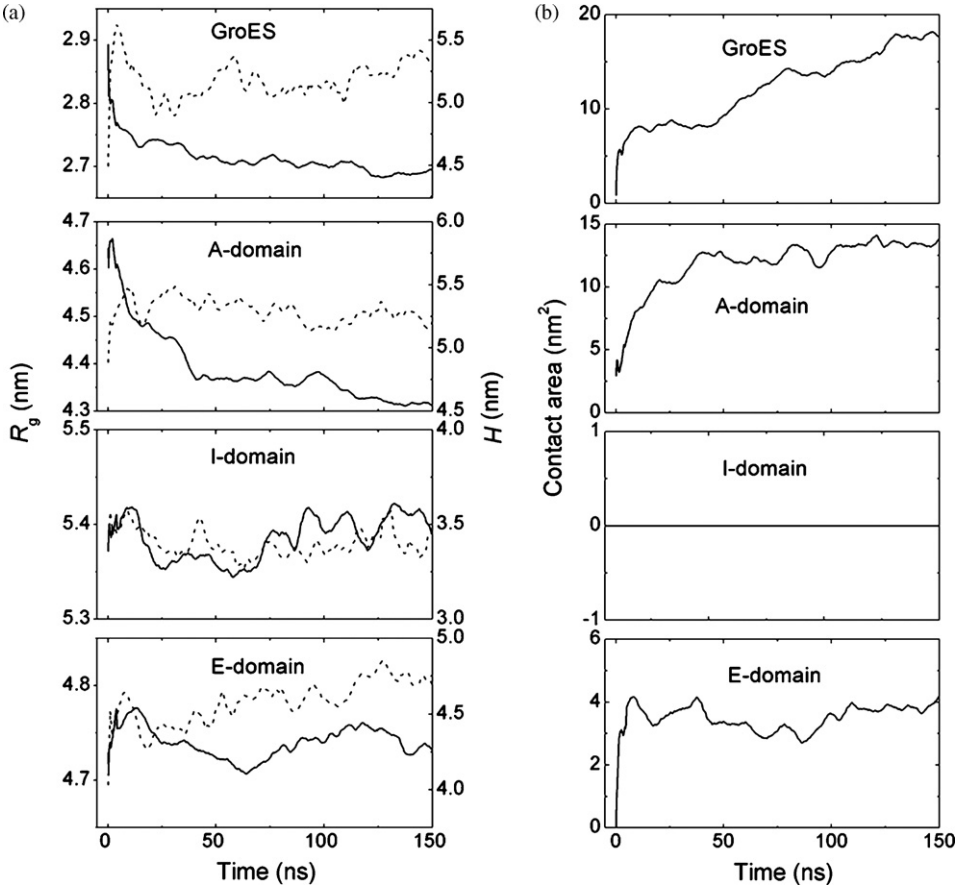

Fig. 2. Plotted as functions of time: (a) R_g (solid line) and H (dash line) of GroES, A-domain, I-domain and E-domain of SR-EL; (b) contact area between the respective domains and rhodanese.

contains four GGM repeats (a GGM repeat consists three consecutive residues of G, G and M) and an additional M residue, which are flexible sequences protruding from the E-domain into the cavity. Compared to wild type (SR-EL), the cavity volume would reduce by ~4.4% through duplication of the $[GGM]_4M$ sequences. Experiments have shown that rhodanese experiences an acceleration of folding rate upon reducing the cage size by ~4.4% for SR-2$[GGM]_4$, and also ~8.7% for SR-3$[GGM]_4$ which slows folding dramatically. Each GroEL subunit has 6 negative charges (residues E251, D252, E254, D358, D360 and E362) in the A-domain, providing the possibility of investigating the effect of cavity charge through their mutation. Two cavity-charge mutants, which result in complete loss of cavity net charge, are particularly noticeable. The negative-to-positive mutant SR-KKK (D358K, D360K and E362K) results in a significant acceleration of folding rate compared to SR-EL, and the negative-to-neutral mutant SR-3N3Q (E251Q, D252N, E254Q, D358N, D360N and E362Q) dramatically slows down rhodanese folding.

2. Simulation methods

Table 1 shows the five individual systems simulated, including the wild type GroEL (SR-EL), two systems with altered cavity size (SR-2$[GGM]_4$ and SR-3$[GGM]_4$) and two systems with altered cavity charge (SR-KKK and SR-3N3Q). Simulations are performed using the GROMACS package (Berendsen, van der Spoel, & van Drunen, 1995) in conjunction with Gromos 96 43A1 force field (Van Gunsteren et al., 1996) and SPC (Berendsen, Postma, van Gunsteren, & Hermans, 1981) water model. Particle Mesh Ewald summation (Ulrich et al., 1995) is adopted for long-range electrostatics, and van der Waals cut-off radius is 1.4 nm. The LINCS algorithm (Hess, 2008) is applied to constrain covalent bonds in the protein. Periodic boundary conditions are applied and sodium ions are added to neutralize the system. The minimum distance between any atom of the proteins and the simulation box is 1.0 nm. The hydrogen atoms are modeled as virtual sites, which are massless interaction sites constructed from nearby atom positions, allowing a time step of 4 fs.

To generate the starting conformation for each system, the following protocol is used. Rhodanese is unfolded by simulation of high-temperature (500 K) denaturing for 1.2 ns. From this simulation, the structure with ~53% of the secondary structures is selected as the initial conformation. A complex of rhodanese and GroEL/ES is constructed by inserting the unfolded rhodanese into the center of the cis-cavity, and care is taken to avoid contact between rhodanese and the GroEL/ES complex. After energy minimization using the steepest descent algorithm, a 60 ps MD simulation with position restraints on GroEL/ES and rhodanese is performed at 308 K to gently relax the system. Unrestrained NPT simulation is then performed using Berendsen's temperature and pressure coupling methods (Berendsen, Postma, van Gunsteren, DiNola, & Haak, 1984) to maintain the system at 308 K and 1 atm.

For each system, we perform parallel computations on a dual-CPU quad-core (8-way) HP xw8600 workstation, the whole simulations taking 7500 CPU days.

3. Results

The progress of rhodanese folding is monitored by calculating three structural parameters over time according to the following criteria:

1. Solvent accessible surface area (SASA) with a probe radius of 0.14 nm.

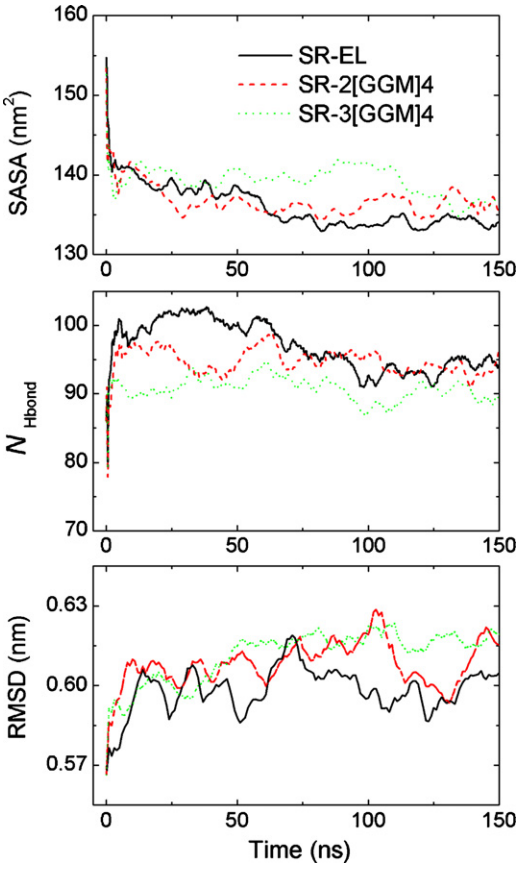

Fig. 3. Rhodanese properties obtained with different GroEL cavity-size mutants during the simulation.

2. Root-mean-square deviation (RMSD) calculation after a least-squares fitting of the structure onto the native conformation which is obtained as an average structure of correctly folded rhodanese in bulk solution at 308 K.
3. Number of hydrogen bonds among the main chain atoms (N_{Hbond}), determined on the basis of donor–acceptor distance smaller than 0.35 nm and of donor–hydrogen-acceptor angle larger than 150°.

3.1. Stability and flexibility of the GroEL/ES complex during rhodanese folding

Folding within the chaperonin cavity is different from folding in bulk solution since the substrate protein is very likely to interact with the inner lining of the cavity, which could also lead to conformational changes of the chaperonin complex. This could be depicted by the contact area between rhodanese and GroES, A-domain, I-domain and E-domain of GroEL and the corresponding structural properties of the GroEL/ES complex as shown in Fig. 2, e.g. radius of gyration to the principal component axis (R_g) and the height along the axis (H). Apparently, GroES and the A-domain of GroEL have strong interactions with rhodanese, as evidenced by the apparent increase in the contact area curves, respectively, while the E-domain has a weak interaction through the flexible C-terminus and the I-domain has no interaction with rhodanese at all. The conformation of each domain of the GroEL/ES complex changes correspondingly, especially the remarkable decrease of the R_g curve and significant variance of the H curve for GroES and the A-domain, suggesting a compro-

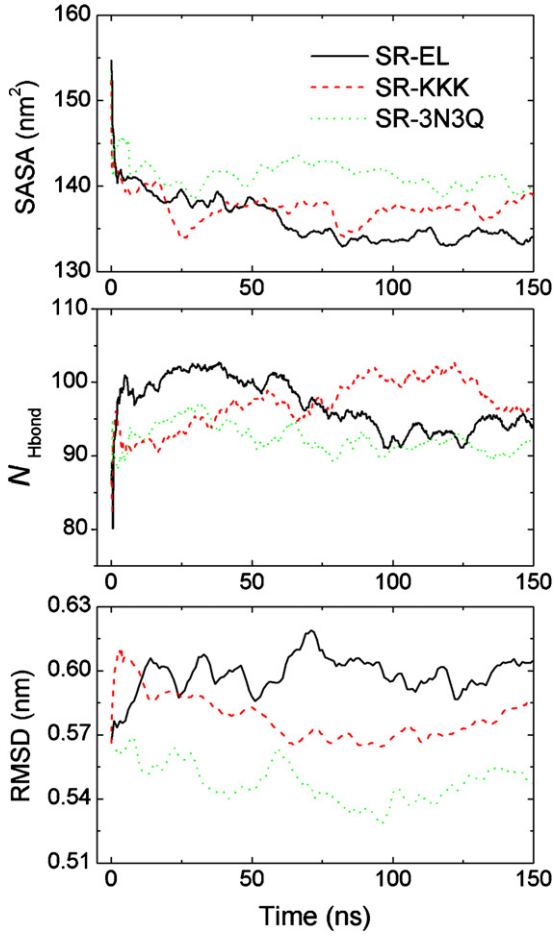

Fig. 4. Rhodanese properties obtained with different GroEL cavity-charge mutants during the simulation.

mise between stability and flexibility during rhodanese folding. The chaperonin complex needs structural stability to maintain the cage structure of the complex, and meanwhile it requires a certain degree of flexibility to demonstrate its biological activity.

3.2. Effect of cavity size on folding

Fig. 3 plots SASA, N_{Hbond} and RMSD against time to depict the kinetics of chaperonin-assisted rhodanese folding. The SASA plot indicates the interfacial properties along the folding process; the N_{Hbond} plot is strongly correlated with the formation of the secondary structures (Clark, 2005); and the RMSD plot depicts the tertiary structural transitions.

Encapsulation of rhodanese in the cavity has dramatically decreased the SASA value of SR-EL and SR-2[GGM]$_4$, approaching the native value of 137.2 nm^2 during the simulation, while the SR-3[GGM]$_4$ system shows slower burial of hydrophobic residues and lesser formation of secondary structures as compared to the other two systems. The RMSD plots suggest that rhodanese experiences an unfolding event throughout the simulation characterized by stepwise increase in SR-3[GGM]$_4$, while SR-EL and SR-2[GGM]$_4$ can assist rhodanese folding through multiple rounds of folding/unfolding events, thus the kinetically trapped intermediates of the substrate formed during the folding process can be partially unfolded and provide with another chance to refold.

3.3. Effect of cavity charge on folding

The SASA curve of SR-KKK in Fig. 4 shows a fast convergence to the value of the native state in 23 ns, and the N_{Hbond} curve shows a dramatic increase of 15 hydrogen bonds in the first 90 ns except for the initial relaxation during the starting 3 ns, suggesting a folding event. This is followed by an unfolding event thereafter characterized by a decrease of eight hydrogen bonds and an increase of 0.015 nm in RMSD but no visible change in SASA. Though the RMSD profile of SR-3N3Q shows a sharp decrease of 0.038 nm in the first 96 ns, the SASA profile shows a delayed burial of hydrophobic residues evidenced by a SASA value much higher than the native state at the end of the simulation, and the N_{Hbond} profile shows a slower formation of secondary structures than the other two systems, indicating a weak ability to assist rhodanese folding.

4. Conclusions

Molecular dynamics (MD) simulations suffer from limited sampling while experiments provide statistical results, and the 150 ns of chaperonin-assisted protein folding is far less than the biological event (~s), thus our results are difficult to be directly compared with the experimental results. However, our investigations have shed some light on the chaperonin-assisted protein folding mystery. The simulation results show that rhodanese folds at the inlet of the central cavity after encapsulation, mainly contacting GroES and the A-domain of GroEL, and it can also extend into the E-domain region of the central cavity. Meanwhile, substrate binding induces remarkable adjustments in the chaperonin itself, observed mainly as clustering together of subunits of GroES and the A-domain of GroEL, forming a tighter enclosure for the substrate. Mutations in either the size or the charge of the cavity can change rhodanese folding properties, probably by altering the contacts between chaperonin and the substrate protein and thus changing the folding pathway. More details are still under investigation and will be published later.

Acknowledgements

This work is supported by the Knowledge Innovation Program of Chinese Academy of Sciences under the Grant Nos. O82811 and KGCX2-YW-124, and National Natural Science Foundation of China under the Grant Nos. 20490201 and 20221603. We wish to thank Prof. Chih-chen Wang and Dr. Xi Wang (National Laboratory of Biomacromolecules, Institute of Biophysics, Chinese Academy of Sciences) for their helpful discussion.

References

Berendsen, H. J. C., Postma, J. P. M., van Gunsteren, W. F., DiNola, A., & Haak, J. R. (1984). Molecular dynamics with coupling to an external bath. *The Journal of Chemical Physics*, *81*, 3684–3690.

Berendsen, H. J. C., Postma, J. P. M., van Gunsteren, W. F., & Hermans, J. (1981). Interaction models for water in relation to protein hydration. In *Intermolecular forces*. Dordrecht: Reidel., pp. 331–342.

Berendsen, H. J. C., van der Spoel, D., & van Drunen, R. (1995). GROMACS: A message-passing parallel molecular dynamics implementation. *Computer Physics Communications*, *91*, 43–56.

Clark, D. P. (2005). *Molecular biology: Understanding the genetic revolution*. New York: Academic Press.

Ellis, R. J. (2001). Molecular chaperones: Inside and outside the Anfinsen cage. *Current Biology*, *11*, 1038–1040.

Ge, W., Chen, F. G., Gao, J., Gao, S. Q., Huang, J., Liu, X. X., et al. (2007). Analytical multi-scale method for multi-phase complex systems in process engineering—Bridging reductionism and holism. *Chemical Engineering Science*, *62*(13), 3346–3377.

Ge, W., & Li, J. H. (2001). Macro-scale pseudo-particle modeling for particle-fluid systems. *Chinese Science Bulletin*, *46*(18), 1503–1507.

Hess, B. (2008). P-LINCS: A parallel linear constraint solver for molecular simulation. *Journal of Chemical Theory and Computation*, *4*, 116–122.

Horowitz, P. M. (1995). Chaperonin-assisted protein folding of the enzyme rhodanese by GroEL/GroES. In *Protein stability and folding: Theory and practice*. New Jersey: Humana Press., pp. 361–368.

Jewett, A. I., Baumketner, A., & Shea, J. E. (2004). Accelerated folding in the weak hydrophobic environment of a chaperonin cavity: Creation of an alternate fast folding pathway. *Proceedings of the National Academy of Sciences*, *101*(36), 13192–13197.

Klimov, D. K., Newfield, D., & Thirumalai, D. (2002). Simulations of beta-hairpin folding confined to spherical pores using distributed computing. *Proceedings of the National Academy of Sciences*, *99*(12), 8019–8024.

Lin, J. H., Baker, N. A., & McCammon, J. A. (2002). Bridging implicit and explicit solvent approaches for membrane electrostatics. *Biophysical Journal*, *83*(3), 1374–1379.

Ploegman, J. H., Drent, G., Kalk, K., & Hol, W. (1978). Structure of bovine liver rhodanese. I. Structure determination at 2.5 Å resolution and a comparison of the conformation and sequence of its two domains. *Journal of Molecular Biology*, *123*(4), 557–594.

Takagi, F., Koga, N., & Takada, S. (2003). How protein thermodynamics and folding mechanisms are altered by the chaperonin cage: Molecular simulations. *Proceedings of the National Academy of Sciences*, *100*(20), 11367–11372.

Tang, Y. C., Chang, H. C., Roeben, A., Wischnewski, D., Wischnewski, N., Kerner, M. J., et al. (2006). Structural features of the GroEL–GroES nano-cage required for rapid folding of encapsulated protein. *Cell*, *125*(5), 903–914.

Ulrich, E., Lalith, P., Max, L. B., Tom, D., Hsing, L., & Lee, G. P. (1995). A smooth particle mesh Ewald method. *The Journal of Chemical Physics*, *103*, 8577–8593.

Van Gunsteren, W. F., Billeter, S. R., Eising, A. A., Hünenberger, P. H., Krüger, P., Mark, A. E., et al. (1996). *Biomolecular simulation: The GROMOS96 manual and user guide*. Zurich: Vdf Hochschulverlag.

Xu, Z., Horwich, A. L., & Sigler, P. B. (1997). The crystal structure of the asymmetric GroEL–GroES–$(ADP)_7$ chaperonin complex. *Nature*, *388*, 741–750.